



Modeling of Lüders elongation and work hardening behaviors of ferrite-pearlite dual phase steels under tension

Bo Mao, Yiliang Liao*

Department of Mechanical Engineering, University of Nevada, Reno, Reno, NV 89557, USA

ARTICLE INFO

Keywords:

Ferrite-pearlite steel
Representative volume element method
Lüders elongation

ABSTRACT

Because of their good combination of strength and ductility, ferrite-pearlite (F-P) dual phase steels are widely used as structural components for various engineering applications. Several numerical models have been developed to predict the flow behavior of F-P steels with a focus on the strain hardening effect. However, little attention has been put on modeling the Lüders elongation phenomenon, which dominates the plastic behavior of F-P steels at a relatively low-strain range. This research is to establish a stress–strain model capable of predicting both the Lüders elongation and work hardening behaviors of F-P steels subjected to room temperature tension. Representative volume element method in combination with finite element simulation is used for the overall stress–strain relationship prediction. The effects of ferrite grain size, pearlite volume fraction, and pearlite inter-lamellar spacing on flow behaviors are investigated. Model validation is achieved by comparing the simulation results with experimental data from literature.

1. Introduction

Ferrite-pearlite (F-P) dual phase steels are widely used as structural components for various engineering applications. This is attributed to their good combination of ductility and strength (Karlsson and Linden, 1975). The relationship between the microstructure and mechanical properties of F-P steels are studied by various experimental and numerical methods (Linaza et al., 1993; Mintz, 1984; Q'Donnely et al., 1984). The key microstructural characteristics responsible for the plasticity of F-P steels include ferrite grain size, pearlite inter-lamellar spacing, and volume fraction of each individual phase (Al-Abbasi, 2013; Allain and Bouaziz, 2008; Wang et al., 2017a). A microstructure-based model capable of bridging those microstructure characteristics with the plasticity of F-P steels is of specific importance.

In literature, several models have been developed to predict the flow behavior of F-P steels. Those modeling methodologies include finite element method (FEM), crystal plasticity approach, and physics-based micromechanical simulation. For instance, Suh et al. (2001) carried out FEM simulation to predict the flow curves of F-P steels through using a microstructural unit cell to represent the phase configuration. Allain and Bouaziz (2008) applied a modified classical mean field approach to predict the tensile behavior and Bauschinger effects of F-P steels. Yamanaka et al. (2008) coupled phase field (PF) simulation with representative volume element (RVE) method to model the

stress–strain relationship of F-P steels. Watanabe et al. (2012) proposed a multiscale analysis method integrating crystal plasticity model with FEM to predict the plasticity of F-P steels.

These aforementioned models have made some progress towards bridging the microstructure and plasticity of F-P steels, particularly for the strain-hardening effect. However, little effort has been put on modeling the Lüders elongation phenomenon, which dominates the plastic behavior of F-P steels at a relatively low-strain range. When a F-P steel is stretched in tension, the initial deformation is mainly elastic together with a very small amount of grain collapse. Once the applied stress reaches a certain value, the local yielding is nucleated in one or more regions (Mao et al., 2018). The cross-sections of the specimen are rapidly encompassed by these yielded regions, leading to the drop of stress from the upper yield point to a value that allows the growth of these yielding bands. As a result, Lüders elongation (discontinuous yielding) phenomenon dominates the plasticity in such a low-strain range. It is well accepted that Lüders elongation in F-P dual phase steels is mainly attributed to the flow behavior of ferrite phase (Lee et al., 2011; Luo et al., 2015; Tsuchida et al., 2008). For ferrite steels, the interstitial atoms clustered around the dislocation structures interfere with dislocation slip, leading to the initial yield strength. With the increase of external stress, dislocations move away from the clusters of interstitial atoms, resulting in the dislocation slip at a lower applied stress (Donald, 2018; Liao et al., 2011). Two typical forms of plastic

* Corresponding author.

E-mail address: yliang@unr.edu (Y. Liao).

<https://doi.org/10.1016/j.mechmat.2018.11.015>

Received 15 May 2018; Received in revised form 21 November 2018; Accepted 28 November 2018

Available online 29 November 2018

0167-6636/ © 2018 Elsevier Ltd. All rights reserved.

instability include the Lüders elongation originated from static strain aging and the Portevin Le-Chatelier effect caused by the dynamic strain aging (Kubin and Estrin, 1985; Sarmah and Ananthkrishna, 2015; Wang et al., 2017b). Previous studies indicate that the ferrite grain size is the key microstructural characteristic determining the Lüders elongation phenomenon in terms of upper and lower yield points and elongation strain (Morrison, 1966). Therefore, for modeling the stress–strain relationship of F-P steels, taking into consideration of Lüders elongation of ferrite phase is critical in order for improving the modeling accuracy particularly at a low-strain range.

Several models have been proposed to predict the Lüders elongation phenomenon. For instance, Hahn proposed a model based on the dislocation multiplication and velocity characteristics to capture the discontinuous yielding phenomenon in irons (Hahn, 1962). Mühlhaus et al. developed a gradient plasticity model for predicting the Lüders band propagation in a material that deforms dominantly by dislocation glide on a single slip system. This model was able to capture the evolution of band width and velocity during plastic deformation (Mühlhaus and Boland, 1991). Mazière et al. developed a constitutive model coupled with FEM to simulate Lüders band propagation in a low carbon ferritic steels. This model was capable of predicting the Lüders band propagation under different loading conditions, such as shearing and tension. However, most of these physics-based models are developed based on Mecking–Kocks theory which focuses on the fundamental relationship between flow stress and dislocation density (Mecking and Kocks, 1981), while little attention was paid on the effects of microstructure characteristics such as phase volume fraction and grain size. To overcome this barrier, a microstructural based model was recently proposed by Johnson et al. (2015). This model was able to predict the magnitude of Lüders strain as affected by carbon content, strain rate, and grain size. However, modeling of strain hardening stage after Lüders elongation was not involved in this work. In our recent study, a microstructure-based ferrite model capable of capturing both the Lüders elongation and work-hardening behaviors was developed (Zhang and Liao, 2016).

In this study, we propose a stress–strain model capable of predicting both the Lüders elongation and work hardening behaviors of F-P steels subjected to room temperature tension. RVE method in combination with finite element simulation is used for the overall stress–strain relationship prediction. The effects of ferrite grain size, pearlite volume fraction, and pearlite inter-lamellar spacing on flow behaviors are investigated. Model validation is achieved by comparing the simulation results with experimental data from literature.

2. Model description

2.1. Modeling of flow behavior of ferrite

Ferrite serves as the soft matrix in the F-P dual phase steels. For the ferrite phase subjected to tension at a low stress level, the interaction between dislocations and interstitial atoms retards the initiation of dislocation slip. Once the applied stress reaches the upper yield point, σ_{UY} , dislocation slips are initiated, leading to local yielding in one or more regions. As a result, dislocations move away from the clusters of the interstitial atoms, and the required stress for dislocations slip drops to a lower yield point, σ_{LY} . The specimen will continue elongation under this lower yield stress until band fronts propagate throughout the entire gage length. After this, the stress–strain relation is dominated by the work-hardening effect due to the multiplication and propagation of dislocations (Zhang and Liao, 2016). Therefore, the stress–strain relationship of ferrite in the plastic region needs to be considered in three continuous stages: Stage I, Lüders elongation behavior at a low-plastic strain; Stage II, early work-hardening behavior in a transition stage at an intermediate strain; and Stage III, work-hardening behavior at a large strain.

In Stage III, since the work-hardening effect of ferrite is mainly attributed to the multiplication and propagation of dislocation structures, the relationship between flow stress σ_e and strain ε can be described as:

$$\sigma = \sigma_0 + \sigma_e = \sigma_0 + \alpha MGb\sqrt{\rho(\varepsilon)}, \quad (1)$$

where σ_0 is the strain-independent stress related to the lattice friction, $G = 80$ GPa is the shear modulus, $M = 3$ is Taylor factor, $\alpha = 1$ is the numerical factor describing dislocation-dislocation interaction, $b = 2.48 \times 10^{-8}$ cm is the Burger's vector, and $\rho(\varepsilon)$ is the dislocation density.

According to Mecking–Kocks theory, the dislocation density evolution with plastic strain can be described as (Mecking and Kocks, 1981):

$$\frac{d\rho(\varepsilon)}{d\varepsilon} = M \left(\frac{1}{bL} - k_2\rho(\varepsilon) \right), \quad (2)$$

where k_2 is the dislocation annihilation rate and L is the dislocation mean free path. For ferrite phase, the magnitude of L is mainly determined by grain boundaries and dislocation-dislocation interactions, and can be expressed as (Bouquerel et al., 2006):

$$\frac{1}{L} = \frac{1}{d} + k_1\rho^{1/2}, \quad (3)$$

where d is the ferrite grain size, and k_1 is the dislocation multiplication rate. The values of k_1 and k_2 are depended on the carbon weight percentage (Zhang and Liao, 2016). Therefore, the strain-hardening behavior of ferrite phase in Stage III can be calculated by:

$$\sigma_e \frac{d\sigma_e}{d\varepsilon} = \frac{M}{2} (k_2\sigma_{ess}^2 + k_1\sigma_{ess}\sqrt{dk_2/b}\sigma_e - k_2\sigma_e^2), \quad (4)$$

where $\sigma_{ess} = \sigma_{0ss} + k_0d^{-0.5}$ is the saturation stress, $\sigma_{0ss} = 232$ MPa and $k_0 = 8.6$ MPa $m^{0.5}$ are constants for Hall-Petch equation (Zhang and Liao, 2016).

For the Lüders elongation phenomenon in Stage I, the hardening effect is negligible as the band propagating at a nearly constant stress, and dislocations near the band front depends on the sustaining band velocity. The flow stress σ can be written as (Hahn, 1962),

$$\sigma = \sigma_e + 2\tau \quad (5)$$

where τ is the resolved shear stress, defined as the minimum stress for the initiation of dislocation, and σ_e is the thermal strain independent work-hardening stress, and can be expressed as $\sigma_e = \frac{1}{2}\alpha GM^2k_1\varepsilon$. According to the Johnston–Gilman Law, the resolved shear stress can be estimated as a function of dislocation velocity v , a constant of n , and the resolved shear stress τ_0 corresponding to the unit velocity (Johnston and Gilman, 1959): $\tau = \tau_0v^{1/n}$. Since the dislocation velocity is strongly affected by the strain rate and dislocation density, it can be estimated as $v = \dot{\varepsilon}/b\rho(\varepsilon)$ (Johnston, 1962; Johnston and Gilman, 1959; Stein and Low, 1960). Therefore, the flow stress in Stage I (where $0 < \varepsilon < \varepsilon_{LY}$) can be expressed as,

$$\sigma(\varepsilon, \dot{\varepsilon}, d) = \frac{1}{2}\alpha GM^2k_1\varepsilon + 2\tau_0 [\dot{\varepsilon}/(b\rho_0 + M\varepsilon/d)]^{1/n} \quad (6)$$

where $\rho_0 = 6 \times 10^7$ cm^{-2} is the initial dislocation density, $n = 35$ is a constant, and $\dot{\varepsilon}$ is the strain rate. The initial resolved shear stress can be estimated as a function of the upper yield strength σ_{UY} , where the plastic strain is equal to zero: $\tau_0 = \frac{1}{2}\sigma_{UY} [\dot{\varepsilon}/(b\rho_0 + \frac{M\sigma_{UY}}{Ed})]^{-1/n}$.

The upper yield strength could be determined by Pickering's equation (Gutiérrez and Altuna, 2008) as $\sigma_{UY} = \sigma_f + 32Mn + 678P + 83Si + 39Cu - 31Cr + 11Mo + 5544(N_{ss} + C_{ss}) + k_{HP}d^{-0.5}$, where $k_{HP} = 18$ MPa $m^{0.5}$ is a constant and $\sigma_f = 65$ MPa is the lattice friction stress. The relationship between the lower yield strength σ_{LY} and Lüders strain ε_{LY} can be described as $\sigma_{LY} = \frac{1}{2}pM^2k_1G \frac{n+1}{n+\varepsilon_{LY}^p}$ (Enomoto and Furubayashi, 1979), where $p = 0.66$ (Zhang and Liao, 2016). In Stage II, where early work-hardening happens in a transition stage at an intermediate strain, the flow behavior can be calculated as:

$$\sigma = \sigma_{LY} + \sigma_{\varepsilon-\varepsilon_{LY}} = \sigma_{LY} + \alpha M G b \sqrt{\rho(\varepsilon - \varepsilon_{LY})} \quad (7)$$

Therefore, by integrating Eqs. (1)–(6), this multi-stage model is capable of capturing both the work-hardening and Lüders elongation behaviors of ferrite as a function of the key microstructure characteristic of grain size.

2.2. Modeling of flow behavior of pearlite

Pearlite serves as the reinforcement phase in F-P dual phase steels. Pearlite has a lamellar structure in which fine layers of ferrite and cementite are piled up repeatedly at sub-micrometer intervals. It is widely accepted that the inter-lamellar spacing plays a critical role in determining the flow behavior of pearlite phase (Dollár et al., 1988; Embury and Fisher, 1966). When the pearlite steel is subjected to tensile loading, the ferrite layers deform plastically after yielding, and the mobile dislocations in the ferrite are confined by ferrite/cementite interfaces and then propagate by Orowan type bowing. Once mobile dislocations are exhausted, double cross-slip plays as the key mechanism for dislocation manipulation and propagation (Misra et al., 2004). In this paper, the modified Bouaziz and Le Corre (2003) model proposed by Hu et al. (2006) is used to describe the flow behavior of pearlite. This modified Bouaziz model is one of the most advanced microstructure-based models describing the plasticity of pearlite, particularly through taking into consideration of contributions from both ferrite and cementite layers in the lamellar structure (Borchers and Kirchheim, 2016; Hu et al., 2006). For the flow behavior of ferrite layers in pearlite steels, the flow stress σ_F and strain ε relationship can be described as:

$$\sigma_F = \begin{cases} E\varepsilon, & \varepsilon < \varepsilon_F^e \\ \sigma_0 + \frac{M\mu b}{\bar{s}}\varepsilon, & \bar{s} = \bar{s}(\bar{s}_0, \varepsilon), \end{cases} \quad (8)$$

where $E=207GPa$ is the elastic modulus, \bar{s}_0 and \bar{s} refers to the initial and average inter-lamellar spacing of pearlite during plastic deformation, ε_F^e is the elastic limit, μ is the shear modulus of ferrite. For pearlite steels under tension, the average inter-lamellar spacing is a function of equivalent plastic strain and initial inter-lamellar: $\bar{s} = \bar{s}_0 e^{-\varepsilon/2}$ (Bouaziz and Le Corre, 2003). On the other hand, for the cementite layers in the lamellar structure of pearlite, the flow stress σ_C can be described as:

$$\sigma_C = \begin{cases} E\varepsilon, & \varepsilon < \varepsilon_C^i \\ \sigma_C^i + (\sigma_C^y - \sigma_C^i)(1 - e^{-g(\varepsilon - \varepsilon_C^i)}), & \varepsilon > \varepsilon_C^i \end{cases}, \quad g = E/(\sigma_C^y - \sigma_C^i), \quad (9)$$

where σ_C^y is the yield strength of cementite, σ_C^i and ε_C^i are the elastic limit and strain of the cementite phase. $\sigma_C^y = 5.2GPa$ and $\sigma_C^i = 700MPa$ and can be referred in Hu et al. (2006). Based on the rule of mixtures, the flow stress of pearlite steel σ_p , considering contributions of both ferrite and cementite layers, can be calculated as:

$$\sigma_p = f_F \sigma_F + f_C \sigma_C, \quad (10)$$

where $f_C = 0.116$ and $f_F = 0.884$ are the volume fractions of cementite and ferrite, respectively (Watanabe et al., 2012).

2.3. Representative volume element modeling of F-P dual phase steel

RVE is a micromechanical modeling method used to study the mechanical behavior of materials containing two or more phases, such as composite materials (Sun and Vaidya, 1996) and dual phase steels (Liedl et al., 2002). Recent studies show that RVE method can be applied to predict plasticity (Paul, 2013a), fracture (Uthaisangskuk et al., 2011), and fatigue (Farukh et al., 2016). Compared to the traditional modeling method such as rule of mixtures, RVE method provides a detailed description of the stress and strain distribution in the deformation process (Amirmaleki et al., 2016). RVE was first proposed by Hill (1963), in which a material sub-domain was used to represent the

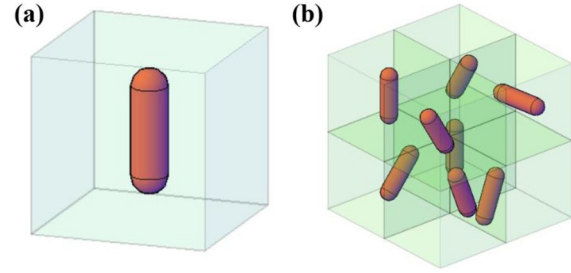


Fig. 1. A schematic view of 3-D RVE model. (a) A unit cell, (b) unit cells aggregation.

microstructure of an alloy in periodic or average sense. A RVE is a unit cell or cells aggregation that has the general characteristics of the materials, such as phase volume fraction, aspect ratio, and phase distribution. Fig. 1a shows a basic 3-D RVE unit cell based on the Mori-Tanaka's approach (Mori and Tanaka, 1973). The cubic and spherocylinder represent the matrix and the second phase, respectively. The size of the cubic and spherocylinder in the unit cell is determined according to the phase volume fraction and the morphology of the second phase. For a dual phase material, a unit cells aggregation model is used to represent the whole microstructure configuration, as shown in Fig. 1b. In recent years, a 3-D RVE model based on real microstructure features are used to predict the flow behavior of dual phase steels (Choi et al., 2013; Paul, 2013b). In this method, microstructure features (in terms of phase volume fraction, and size and aspect ratio of second phase) observed by microscopy images are firstly converted into a RVE model, and then the stress-strain relationship is predicted using FEM simulation.

Fig. 2 shows the computational cells and FEM details used for RVE modeling of stress-strain relationship of F-P steels. A cuboid ferrite matrix which consists of spherical-cylinder inclusions representing the pearlite phase is built using Digimat software (e-Xstream engineering, Louvain-la-Neuve, Belgium) (Fig. 2a). The spherical-cylinder inclusions (marked in red color) are randomly distributed in the matrix. The geometry of the cuboid and the amount of the spherical-cylinder is fixed and the geometry of the inclusions are adjusted according to the pearlite volume fraction. 30 inclusions are incorporated into the matrix to ensure that the RVE computational cell is large enough to capture the global microstructure characteristics. Considering that for the cold rolled F-P steels, the distribution of the pearlite phase typically aligns with the rolling direction; all inclusions in the computational matrix are aligned in one direction. This geometry is then employed as the input of ABAQUS (Hibbit and Sorensen, 2001) for FEM analysis. Fig. 2b shows the loading condition. A constant strain rate of 5×10^{-4} /s is applied at right side of the assembly till reaching a strain of 0.12. For simplification, the interface property of the two phases is defined to be perfectly bonded. C3D10M element type with an initial seed size of 0.05 is used to discretize the whole RVE (Fig. 2c). Macroscopic engineering stresses are obtained by dividing the reaction forces along the x direction by the corresponding initial cross sectional areas. Macroscopic engineering strains are obtained by dividing the right surface displacements by the initial dimensions of the RVE along x direction.

3. Model result, validation and discussion

In this work, the modeling results are validated by experimental data in literature. Table 1 summarizes details of F-P steels used for validation (Suh et al., 2001; Tsuchida et al., 2015).

Fig. 3a and b shows the modeled flow behaviors of individual ferrite and pearlite phases for steels A and B. It can be noted that both the Lüders elongation and strain-hardening behaviors of the ferrite phase can be captured using Eq. (1)–(6). The ferrite phase in steel A exhibits a lower yield strength of 222.9 MPa at a strain of 0.033, while the ferrite

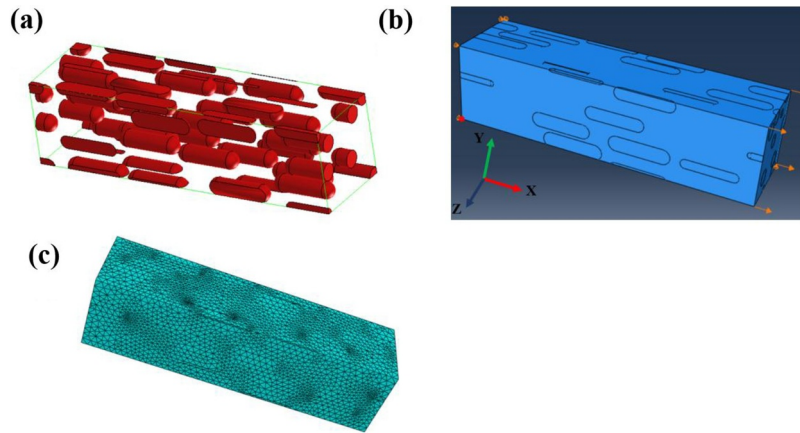


Fig. 2. RVE modeling of F-P steels: (a) Computational cells based on microstructure of F-P steels, (b) Loading and constraining conditions for FEM analysis, and (c) C3D10M mesh for analysis.

Table 1
Chemical composition and microstructure parameters of F-P steels.

Steels	Chemical compositions (%)					Microstructure parameters			Refs.
	C	Si	Mn	P	S	$d(\mu\text{m})$	$s(\text{nm})$	f_p	
A	0.15	0.21	0.5	0.012	0.008	22.6	120	0.18	(Suh et al., 2001)
B	0.15	0.25	1.3	0.012	0.005	20.4	100	0.24	(Suh et al., 2001)
C	0.15	0.4	1.5	0.014	0.004	3.6	130	0.188	(Tsuchida et al., 2015)
D	0.15	0.39	1.35	0.016	0.004	9.8	140	0.12	(Tsuchida et al., 2015)
E	0.15	0.4	1.5	0.014	0.004	36.2	80	0.12	(Tsuchida et al., 2015)

d : ferrite grain size, s : inter-lamellar spacing of pearlite phase, f_p : pearlite volume fraction.

phase in steel B has a lower yield strength of 284.5 MPa at a strain of 0.062. The increase of the lower yield strength and Lüders elongation strain of the ferrite phase for steel B as compared to steel A is attributed to the decrease of ferrite grain size from 22.6 to 20.4 μm . During the tensile test, a smaller grain size promotes the dislocation-dislocation interactions, leading to an enhanced dislocation pinning effect which hinders the dislocation slip. With further tensile loadings these pinned dislocations overcome obstacles and slip until pinned again by obstacles, resulting in the prolongation of Lüders elongation (Butler, 1962; Tsuchida et al., 2006). Moreover, as compared to other modeling works in literature which only emphasize on the Lüders elongation (Mazière and Forest, 2015; Mazière et al., 2017; Mühlhaus and Boland, 1991), the model in the current study captures both the Lüders elongation and work hardening behavior of ferrite phase, thus enables us to predict the whole stress–strain curve of F-P steels.

In addition, the flow behaviors of pearlite for steels A and B are predicted using Eq. (7)–(9) (Fig. 3a and b). It is observed that a finer pearlite inter-lamellar spacing leads to a higher stress level. For instance, as the inter-lamellar spacing decreases from 120 to 80 nm, the yield strength of the pearlite increases from 730.2 to 816.3 MPa.

As compared to models available in literature, this model using RVE method in combination with FEM simulation can reveal the evolution of stress distribution in F-P steels during monotonic tension. The simulation results of Fig. 3 are implemented into RVE model for prediction of the stress–strain relationship of F-P dual phase steel. Fig. 4 shows the contour plots of the Von Mises stress distribution of steels A and B at a strain 0.02, 0.04, and 0.10 as predicted by RVE model. The stress distribution in each individual phase is revealed. A heterogeneous stress distribution can be clearly observed, and the degree of heterogeneity of stress increases with the increase of strain. Moreover, it can be noted

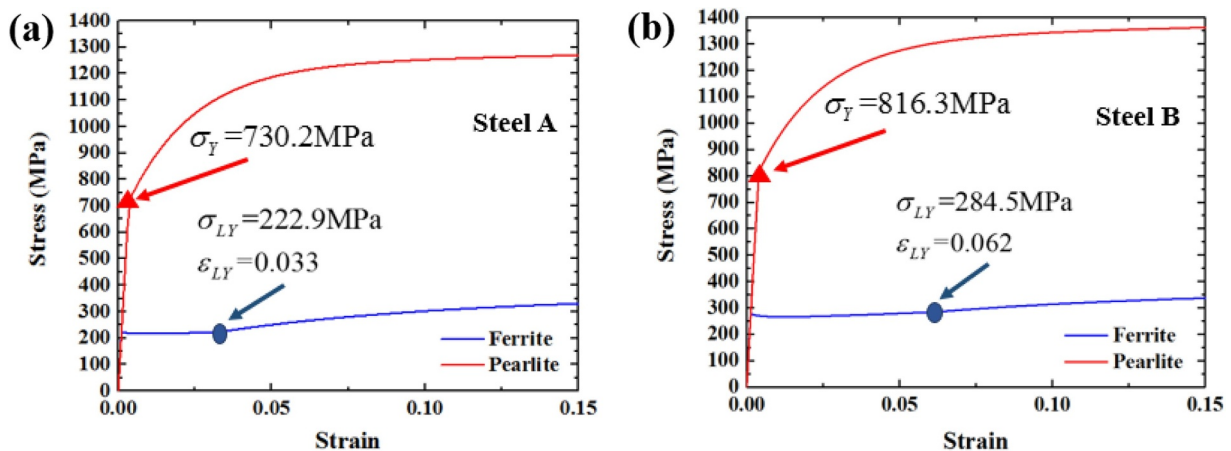


Fig.3. Molded flow behaviors of ferrite and pearlite phase for steels A and steel B, (a) Steel A and (b) Steel B.

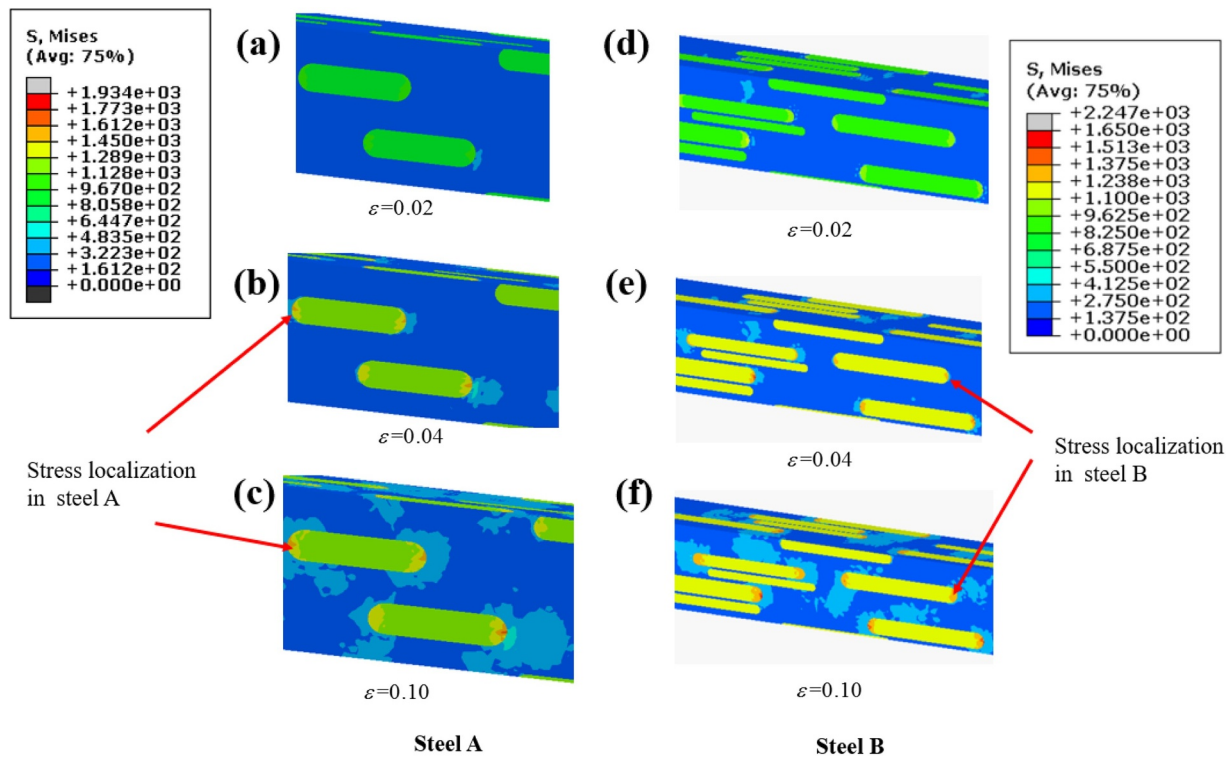


Fig. 4. Von Mises stress distribution during the deformation process of F-P steels A and B by FE analysis at various strain levels of (a) $\epsilon = 2\%$, (b) $\epsilon = 4\%$, (c) $\epsilon = 10\%$ for steel A, (d) $\epsilon = 2\%$, (e) $\epsilon = 4\%$ and (f) $\epsilon = 10\%$ for steel B.

that stress localization often develops at the ferrite-pearlite interface, as indicated by the red arrows. With the increase of strain, the stress localization propagates into the ferrite phase. Similar results have also been reported by previous studies (Sodjit and Uthaisangskuk, 2012). This stress concentration is due to the mismatch of the mechanical properties between the neighboring grains, which causes the debonding of the two different phases. Further stress concentration finally leads to the void formation and failure of the F-P dual phase steels (Komori, 2014).

The simulated stress–strain curves of steels A and B are compared with experimental data (Suh et al., 2001) as shown in Fig. 5. The modeling results show a good agreement with the experimental data. In particular, both the Lüders elongation phenomenon and strain hardening effect are captured. It can be seen that the modeled lower yield strengths are 322 MPa for steel A (at a strain of 0.022) and 408.3 MPa for steel B (at a strain of 0.048), which match well with the experimental results. The predicted flow stresses at the work-hardening stages

for steels A and B are slightly higher than the experimental data. Note that the modeling accuracy for F-P dual phase steels is determined by not only the prediction of flow behaviors of individual phase, but also the consideration of ferrite-pearlite interface. In the proposed RVE model, the two different phases are assumed to be perfectly bonded and deform simultaneously as subjected to external loadings (Han et al., 2005; Iza-Mendia and Gutiérrez, 2013). On the other hand, in the real experimental tests, the ferrite phase yields first while the pearlite phase remains elastic since the yield stress of the pearlite is much higher than the ferrite (Rivera-Diaz-Del-Castillo et al., 2004). Therefore, the flow strength of F-P steels at a low strain range is mainly dominated by the flow behavior of ferrite phase. In the proposed RVE model, the assumption that two phases deform simultaneously leads to a slightly higher strength level as compared to experimental data, since both contributions from ferrite and pearlite phases are considered at the early stage of plastic deformation.

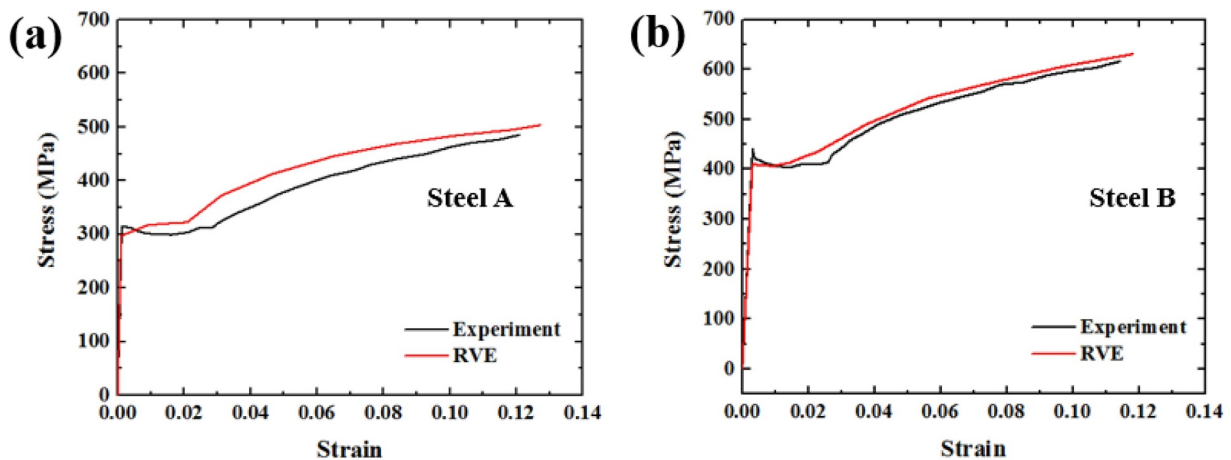


Fig. 5. Comparisons between experimental and RVE modeled stress–strain relationship of investigated F-P steels: (a) Steel A and (b) Steel B.

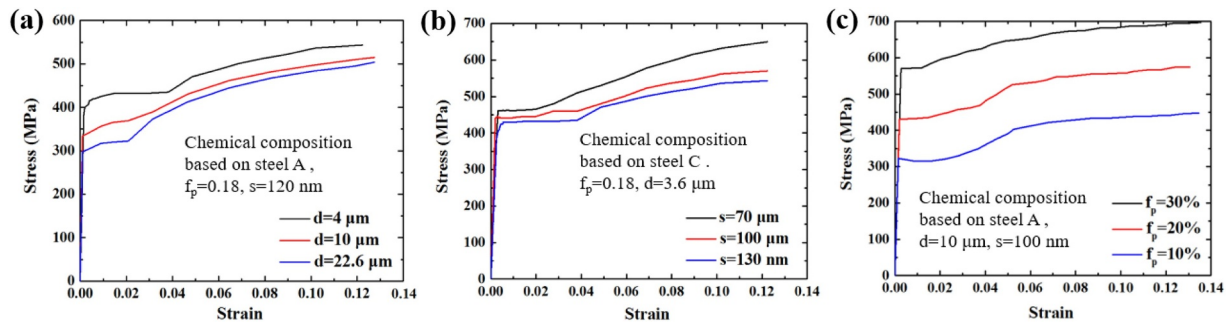


Fig. 6. The effect of microstructure on the flow behaviors of F-P steels. Predicted stress–strain relationship of F-P steels as affected by (a) The ferrite grain sizes, (b) The pearlite inter-lamellar spacing, and (c) The pearlite volume fractions.

More importantly, a key advantage of the proposed model is the capability of predicting the microstructure effect on the flow behavior of F-P steels. The predicted stress–strain relationships of F-P steels as affected by the ferrite grain sizes, pearlite inter-lamellar spacing, and pearlite volume fractions are shown in Fig. 6a, b, and c, respectively. A constant strain rate of 0.0005/s is applied for simulations. As observed in Fig. 6a, given the same chemical composition as steel A, a pearlite volume fraction of 18%, and a pearlite inter-lamellar spacing of 120 nm, both the lower yield strength and Lüders elongation strain increase with the decrease of ferrite grain size. For instance, as the ferrite grain size decreases from 22.6 μm to 4 μm , the lower yield strength increases from 326.5 MPa to 414.5 MPa, and the Lüders elongation strain increases from 0.023 to 0.041. For ferrite phase, the dislocation mean free path is mainly determined by the ferrite grain size. A smaller ferrite grain size leads to enhanced dislocation pinning strength, therefore, a higher strength level. The increase of Lüders elongation strain with the decrease of ferrite grain size is also consistent with the results in other modeling works and experimental observation (Gutiérrez and Altuna, 2008; Johnson et al., 2015; Luo et al., 2015). For example, the model proposed by Johnson et al. (2015) indicated that $\epsilon_{LY} \propto d^{-1/2}$, where d is the ferrite grain size.

The effect of pearlite inter-lamellar spacing on flow behavior of F-P steels is shown in Fig. 6b. Given the same chemical composition as steel C, a pearlite volume fraction of 18%, and ferrite grain size of 3.6 μm , the lower yield strength increases and the Lüders elongation strain decreases with the decrease of pearlite inter-lamellar spacing. For instance, as the pearlite inter-lamellar spacing decreases from 130 to 70 nm, the lower yield strength of the F-P steel increases from 427 MPa to 468 MPa, and the Lüders elongation strain decreases from 0.041 to 0.032. For pearlite structure, the interlamellar spacing serves as the key factor determining the dislocation mean free path. A smaller inter-lamellar spacing leads to a shorter dislocation mean free path for enhanced dislocation pinning effect, leading to a higher strength level (Allain and Bouaziz, 2008). In addition, the proposed RVE model is capable of capturing the effect of pearlite volume fraction as shown in Fig. 6c. Given the same chemical composition as steel A, a ferrite grain size of 10 μm , and a pearlite inter-lamellar spacing of 100 nm, a larger

pearlite volume fraction leads to a higher flow stress level and a smaller Lüders elongation strain. For instance, as the pearlite volume fraction increases from 10% to 30%, the lower yield strength of the F-P steels increases from 357.6 MPa to 572.0 MPa, while the Lüders elongation strain decreases from 0.052 to 0.018. Similar results have also been reported in previous literature (Gladshstein et al., 2012; Watanabe et al., 2012). With the increased volume fraction of pearlite, the flow behavior of F-P steels will be dominated stress–strain relationship of pearlite, leading to a higher yield strength and a lower Lüders elongation strain.

With the inputs of microstructure characteristics, further model validation is shown in Fig. 7. It is observed that RVE modeling results show a relatively good agreement with experimental data. Both strain hardening and Lüders elongation for steels C–E are captured using the proposed RVE model. Moreover, comparing steels C and D (Fig. 7a and b), given a pearlite inter-lamellar spacing around 0.13 μm , the decrease of pearlite volume fraction and increase of ferrite grain size result in a lower stress level and a smaller Lüders elongation strain. In particular, by increasing ferrite grain size from 3.6 to 9.8 μm and decreasing pearlite volume fraction from 19% to 12%, the lower yield strength decreases from around 400 to 300 MPa and Lüders elongation strain decreases from 0.038 to 0.015. As comparing steels D and E (Fig. 7b and c), steel D exhibits a higher yield strength and a longer Lüders elongation although steel E has a finer pearlite inter-lamellar spacing. Since the ferrite volume fractions in steels D and E are over 80%, ferrite grain size effect serves as the domination microstructure characteristics determining the stress–strain relationship. The grain refinement of ferrite phase leads to the improved upper and lower yield strength due to Hall-Petch relationship, as well as the prolonged Lüders elongation due to enhanced dislocation pinning effect which hinders dislocation slips by smaller grain sizes (Zhang and Liao, 2016).

For F-P dual phase steels, the ferrite grain size, pearlite inter-lamellar spacing, and pearlite volume fraction are strongly affected by manufacturing processes such as the heat treatment procedures (Erdogan, 2002). Therefore, this model has a great potential on bridging manufacturing processes- microstructure-property relationship of F-P dual phase steels. Furthermore, the methodology of RVE modeling utilized in this paper will be applicable to microstructure-based

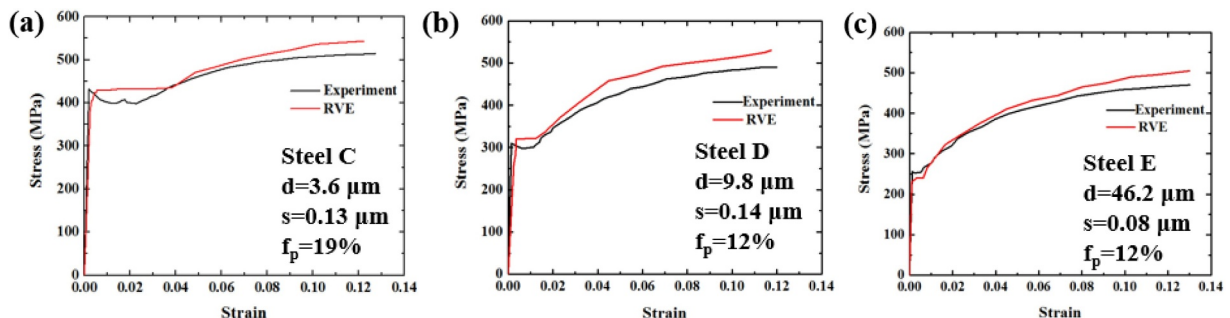


Fig. 7. Comparisons between experimental and RVE modeled stress–strain relationships of (a) Steel C, (b) Steel D, and (c) Steel E.

modeling of structural and engineering steels with complex microstructures, such as ferrite-martensite dual phase steels and TRIP steels.

4. Conclusions

In this paper, a microstructure based stress–strain model is developed to predict both the Lüders elongation and work hardening behaviors of F-P dual phase steels subjected to room temperature tension. RVE method in combination with FEM simulation is used for the overall stress–strain relationship prediction. The major conclusions can be summarized as following:

- (1) This model is capable of predicting Lüders elongation and work hardening behaviors of F-P dual phase steels. In specific, the upper yield strength, lower yield strength, Lüders elongation strain can be revealed from the predicted flow curves as affected by the microstructural characteristics of ferrite grain size, pearlite volume fraction, and pearlite inter-lamellar spacing. The modeling results are validated by experimental data.
- (2) RVE method in combination with FEM simulation reveals the evolution of stress distribution in F-P steels during monotonic tension. A heterogeneous stress distribution can be identified, and the degree of heterogeneity of stress increases with the increase of strain. The localized stress concentration develops at the ferrite-pearlite interface and propagates into the ferrite phase.
- (3) Effects of ferrite grain size, pearlite volume fraction, and pearlite inter-lamellar spacing on the stress–strain relationship of F-P steels are captured by this model. Both the lower yield strength and Lüders elongation strain increase with the decrease of ferrite grain size. The lower yield strength increases and Lüders elongation strain decreases with the decrease of pearlite inter-lamellar spacing. A larger pearlite volume fraction leads to a higher flow stress level and a smaller Lüders elongation strain.

It is expected that this model can serve as a promising tool for analysis of process-microstructure-property relationship of F-P dual phase steels. The methodology of RVE modeling utilized in this paper will be applicable to microstructure-based modeling of other structural and engineering steels with complex microstructures, such as ferrite-martensite dual phase steels and TRIP steels.

Acknowledgments

The authors appreciate the financial support by startup funding from the Department of Mechanical Engineering at the University of Nevada, Reno.

Reference

Al-Abbasi, F., 2013. Predicting the deformation behavior of ferrite–pearlite steels using micro mechanical modeling of cells. *Mech. Mater.* 63, 48–64.

Allain, S., Bouaziz, O., 2008. Microstructure based modeling for the mechanical behavior of ferrite–pearlite steels suitable to capture isotropic and kinematic hardening. *Mater. Sci. Eng. A* 496, 329–336.

Amirmaleki, M., Samei, J., Green, D.E., van Riemsdijk, I., Stewart, L., 2016. 3D micro-mechanical modeling of dual phase steels using the representative volume element method. *Mech. Mater.* 101, 27–39.

Borchers, C., Kirchheim, R., 2016. Cold-drawn pearlitic steel wires. *Prog. Mater. Sci.* 82, 405–444.

Bouaziz, O., Le Corre, C., 2003. Flow stress and microstructure modelling of ferrite-pearlite steels during cold rolling. *Mater. Sci. Forum* 426–432, 1399–1404.

Bouquerel, J., Verbeke, K., De Cooman, B., 2006. Microstructure-based model for the static mechanical behaviour of multiphase steels. *Acta Mater.* 54, 1443–1456.

Butler, J., 1962. Lüders front propagation in low carbon steels. *J. Mech. Phys. Solids* 10, 313–318.

Choi, S.-H., Kim, E.-Y., Woo, W., Han, S., Kwak, J., 2013. The effect of crystallographic orientation on the micromechanical deformation and failure behaviors of DP980 steel during uniaxial tension. *Int. J. Plast.* 45, 85–102.

Dollar, M., Bernstein, I., Thompson, A., 1988. Influence of deformation substructure on flow and fracture of fully pearlitic steel. *Acta Metall.* 36, 311–320.

Donald, R.A., 2018. *Essentials of Materials Science and Engineering*. Cengage Learning SI

edition.

Embury, J.D., Fisher, R.M., 1966. The structure and properties of drawn pearlite. *Acta Metall.* 14, 147–159.

Enomoto, M., Furubayashi, E., 1979. A model for Lüders band formation and plastic instability in iron related with the strain softening due to the Johnston-Gilman-Hahn theory. *Scr. Metall.* 13, 113–117.

Erdogan, M., 2002. The effect of new ferrite content on the tensile fracture behaviour of dual phase steels. *J. Mater. Sci.* 37, 3623–3630.

Farukh, F., Zhao, L., Jiang, R., Reed, P., Proppentner, D., Shollock, B., 2016. Realistic microstructure-based modelling of cyclic deformation and crack growth using crystal plasticity. *Comput. Mater. Sci.* 111, 395–405.

Gladshstein, L., Larionova, N., Belyaev, B., 2012. Effect of ferrite-pearlite microstructure on structural steel properties. *Metallurgist* 56, 579–590.

Gutiérrez, I., Altuna, M., 2008. Work-hardening of ferrite and microstructure-based modelling of its mechanical behaviour under tension. *Acta Mater.* 56, 4682–4690.

Hahn, G.T., 1962. A model for yielding with special reference to the yield-point phenomena of iron and related bcc metals. *Acta Metall.* 10, 727–738.

Han, K., Van Tyne, C., Levy, B., 2005. Effect of strain and strain rate on the Bauschinger effect response of three different steels. *Metall. Mater. Trans. A* 36, 2379–2384.

Hibbitt, Karlsson, Sorensen, 2001. *ABAQUS/Standard User's Manual*. Hibbitt, Karlsson & Sorensen.

Hill, R., 1963. Elastic properties of reinforced solids: some theoretical principles. *J. Mech. Phys. Solids* 11, 357–372.

Hu, X., Van Houtte, P., Liebherr, M., Walentek, A., Seefeldt, M., Vandekinderen, H., 2006. Modeling work hardening of pearlitic steels by phenomenological and Taylor-type micromechanical models. *Acta Mater.* 54, 1029–1040.

Iza-Mendia, A., Gutiérrez, I., 2013. Generalization of the existing relations between microstructure and yield stress from ferrite–pearlite to high strength steels. *Mater. Sci. Eng. A* 561, 40–51.

Johnson, D., Edwards, M., Chard-Tuckey, P., 2015. Microstructural effects on the magnitude of Lüders strains in a low alloy steel. *Mater. Sci. Eng. A* 625, 36–45.

Johnston, W.G., 1962. Yield points and delay times in single crystals. *J. Appl. Phys.* 33, 2716–2730.

Johnston, W.G., Gilman, J.J., 1959. Dislocation velocities, dislocation densities, and plastic flow in lithium fluoride crystals. *J. Appl. Phys.* 30, 129–144.

Karlsson, B., Linden, G., 1975. Plastic deformation of ferrite–pearlite structures in steel. *Mater. Sci. Eng.* 17, 209–219.

Komori, K., 2014. Proposal and use of a void model for inclusion cracking for simulating inner fracture defects in drawing of ferrite–pearlite steels. *Mech. Mater.* 77, 98–109.

Kubin, L., Estrin, Y., 1985. The Portevin-Le Chatelier effect in deformation with constant stress rate. *Acta Metall.* 33, 397–407.

Lee, S., Lee, S.-J., Kumar, S.S., Lee, K., De Cooman, B., 2011. Localized deformation in multiphase, ultra-fine-grained 6 pct Mn transformation-induced plasticity steel. *Metall. Mater. Trans. A* 42, 3638–3651.

Liao, Y., Ye, C., Gao, H., Kim, B.-J., Suslov, S., Stach, E.A., Cheng, G.J., 2011. Dislocation pinning effects induced by nano-precipitates during warm laser shock peening: dislocation dynamic simulation and experiments. *J. Appl. Phys.* 110, 023518.

Liedl, U., Traint, S., Werner, E., 2002. An unexpected feature of the stress–strain diagram of dual-phase steel. *Comput. Mater. Sci.* 25, 122–128.

Linaza, M., Romero, J., Rodriguez-Ibabe, J., Urcola, J., 1993. Influence of the microstructure on the fracture toughness and fracture mechanisms of forging steels microalloyed with titanium with ferrite-pearlite structures. *Scr. Metall. Et Mater.* 29, 451–456.

Luo, H., Dong, H., Huang, M., 2015. Effect of intercritical annealing on the Lüders strains of medium Mn transformation-induced plasticity steels. *Mater. Des.* 83, 42–48.

Mao, B., Siddaiah, A., Menezes, P.L., Liao, Y., 2018. Surface texturing by indirect laser shock surface patterning for manipulated friction coefficient. *J. Mater. Process. Technol.* 257, 227–233.

Mazière, M., Forest, S., 2015. Strain gradient plasticity modeling and finite element simulation of Lüders band formation and propagation. *Contin. Mech. Thermodyn.* 27, 83–104.

Mazière, M., Luis, C., Marais, A., Forest, S., Gaspérini, M., 2017. Experimental and numerical analysis of the Lüders phenomenon in simple shear. *Int. J. Solids Struct.* 106, 305–314.

Mecking, H., Kocks, U., 1981. Kinetics of flow and strain-hardening. *Acta Metall.* 29, 1865–1875.

Mintz, B., 1984. Influence of cooling rate from normalizing temperature and tempering on strength of ferrite–pearlite steels. *Metals Technol.* 11, 52–60.

Misra, A., Hirth, J., Hoagland, R., Embury, J., Kung, H., 2004. Dislocation mechanisms and symmetric slip in rolled nano-scale metallic multilayers. *Acta Mater.* 52, 2387–2394.

Mori, T., Tanaka, K., 1973. Average stress in matrix and average elastic energy of materials with misfitting inclusions. *Acta Metall.* 21, 571–574.

Morrison, W., 1966. The effect of grain size on the stress–strain relationship in low-carbon steel. *ASM Trans. Q.* 59, 824–846.

Mühlhaus, H.-B., Boland, J., 1991. A gradient plasticity model for Lüders band propagation. *Pure Appl. Geophys.* 137, 391–407.

Paul, S.K., 2013a. Effect of martensite volume fraction on stress triaxiality and deformation behavior of dual phase steel. *Mater. Des.* 50, 782–789.

Paul, S.K., 2013b. Real microstructure based micromechanical model to simulate microstructural level deformation behavior and failure initiation in DP 590 steel. *Mater. Des.* 44, 397–406.

Q'Donnelly, B., Reuben, R., Baker, T., 1984. Quantitative assessment of strengthening parameters in ferrite-pearlite steels from microstructural measurements. *Metals Technol.* 11, 45–51.

Rivera-Diaz-Del-Castillo, P., Van Der Zwaag, S., Sietsma, J., 2004. A model for ferrite/

- pearlite band formation and prevention in steels. *Metall. Mater. Trans. A* 35, 425–433.
- Sarmah, R., Ananthakrishna, G., 2015. Correlation between band propagation property and the nature of serrations in the Portevin–Le Chatelier effect. *Acta Mater.* 91, 192–201.
- Sodjit, S., Uthaisangsk, V., 2012. Microstructure based prediction of strain hardening behavior of dual phase steels. *Mater. Des.* 41, 370–379.
- Stein, D.F., J., Low, 1960. Mobility of edge dislocations in silicon-iron crystals. *J. Appl. Phys.* 31, 362–369.
- Suh, D.-W., Bae, J.-H., Cho, J.-Y., Oh, K.H., Lee, H.-C., 2001. FEM modeling of flow curves for ferrite/pearlite two-phase steels. *ISIJ Int.* 41, 782–787.
- Sun, C., Vaidya, R., 1996. Prediction of composite properties from a representative volume element. *Compos. Sci. Technol.* 56, 171–179.
- Tsuchida, N., Inoue, T., Nakano, H., Okamoto, T., 2015. Enhanced true stress–true strain relationships due to grain refinement of a low-carbon ferrite–pearlite steel. *Mater. Lett.* 160, 117–119.
- Tsuchida, N., Masuda, H., Harada, Y., Fukaura, K., Tomota, Y., Nagai, K., 2008. Effect of ferrite grain size on tensile deformation behavior of a ferrite-cementite low carbon steel. *Mater. Sci. Eng. A* 488, 446–452.
- Tsuchida, N., Tomota, Y., Nagai, K., Fukaura, K., 2006. A simple relationship between Lüders elongation and work-hardening rate at lower yield stress. *Scr. Mater.* 54, 57–60.
- Uthaisangsk, V., Muenstermann, S., Prah, U., Bleck, W., Schmitz, H.-P., Pretorius, T., 2011. A study of microcrack formation in multiphase steel using representative volume element and damage mechanics. *Comput. Mater. Sci.* 50, 1225–1232.
- Wang, L., Tang, D., Song, Y., 2017a. Prediction of mechanical behavior of ferrite-pearlite steel. *J. Iron Steel Res. Int.* 24, 321–327.
- Wang, X., Wang, L., Huang, M., 2017b. Kinematic and thermal characteristics of Lüders and Portevin–Le Chatelier bands in a medium Mn transformation-induced plasticity steel. *Acta Mater.* 124, 17–29.
- Watanabe, I., Setoyama, D., Nagasako, N., Iwata, N., Nakanishi, K., 2012. Multiscale prediction of mechanical behavior of ferrite–pearlite steel with numerical material testing. *Int. J. Numer. Methods Eng.* 89, 829–845.
- Yamanaka, A., Takaki, T., Tomita, Y., 2008. Coupled simulation of microstructural formation and deformation behavior of ferrite–pearlite steel by phase-field method and homogenization method. *Mater. Sci. Eng. A* 480, 244–252.
- Zhang, Z., Liao, Y., 2016. Multi-stage modeling of Lüders elongation and work-hardening behaviors of ferrite steels under tension. *Metall. Mater. Trans. A* 47, 1621–1628.